GEOLOGICAL FIELDWORK

Geology and metamorphic conditions in rocks of the Cassiar Terrane, Glenlyon map area (105L/1), south-central Yukon
R. Black, K. Gladwin and S.T. Johnston 65

Harzburgite Peak: A large mantle tectonite massif in ophiolite from southwest Yukon
D. Canil and S.T. Johnston 77

Yukon Targeted Geoscience Initiative, Part 1: Results of accelerated bedrock mapping in Glenlyon (105L/1-7, 11-14) and northeast Carmacks (115I/9,16) areas, central Yukon
M. Colpron, D.C. Murphy, J.L. Nelson, C.F. Roots, K. Gladwin, S.P. Gordey and J.G. Abbott 85

Yukon Targeted Geoscience Initiative, Part 2: Glacial history, till geochemistry and new mineral exploration targets in Glenlyon and eastern Carmacks map areas, central Yukon
J.D. Bond, A. Plouffe and K. Gladwin 109

Bedrock geology at the boundary between Yukon-Tanana and Cassiar terranes, Truitt Creek map area (NTS 105L/1), south-central Yukon
K. Gladwin, M. Colpron, R. Black and S.T. Johnston 135

Geology of the Dezadeash Range and adjacent northern Coast Mountains (115A), southwestern Yukon: Re-examination of a terrane boundary
J.E. Mezger 149

Geological and U-Pb age constraints on base and precious metal vein systems in the Mount Nansen area, eastern Dawson Range, Yukon
J.K. Mortensen, V.L. Appel and C.J.R. Hart 165

Nature and origin of copper-gold mineralization at the Minto and Williams Creek deposits, west-central Yukon: Preliminary investigations
J.K. Mortensen and R. Tafti 175

Cirque forms and alpine glaciation during the Pleistocene, west-central Yukon
F.E.N. Nelson and L.E. Jackson, Jr 183

Geology and U-Pb zircon geochronology of upper Dorsey assemblage near the TBMB claims, upper Swift River area, southern Yukon
C. Roots, T. Liverton and L. Heaman 199

Preliminary geology of the southern Semenof Hills, central Yukon (105E/1,7,8)
R.-L. Simard and F. Devine 213

Geology and mineral occurrences of the Quartet Lakes map area (NTS 106E/1), Wernecke and Mackenzie mountains, Yukon
D.J. Thorkelson, J.R. Laughton, J.A. Hunt and T. Baker 223

Age of the gold-bearing White Channel Gravel, Klondike district, Yukon
J.A. Westgate, A.S. Sandhu, S.J. Preece and D.G. Froese 241

Plants, bugs, and a giant mammoth tusk: Paleoecology of Last Chance Creek, Yukon Territory
G.D. Zazula, D.G. Froese, A.M. Telka, R.W. Mathewes and J.A. Westgate 251

Geology and metamorphic conditions in rocks of the Cassiar Terrane, Glenlyon map area (105L/1), south-central Yukon

Robin Black[1], Kaesy Gladwin[2] and Stephen T. Johnston[3]
School of Earth and Ocean Sciences, University of Victoria[4]

Black, R., Gladwin, K. and Johnston, S.T., 2003. Geology and metamorphic conditions in rocks of the Cassiar Terrane, Glenlyon map area (105L/1), south-central Yukon. *In:* Yukon Exploration and Geology 2002, D.S. Emond and L.L. Lewis (eds.), Exploration and Geological Services Division, Yukon Region, Indian and Northern Affairs Canada, p. 65-76.

ABSTRACT

Lower Paleozoic miogeoclinal calcareous rocks of the Cassiar Terrane are intruded by the Early Cretaceous Glenlyon Batholith. Garnet-biotite and garnet-muscovite-biotite-aluminum silicate-quartz geothermobarometry on the intrusive wall rocks indicate metamorphism to lower amphibolite facies at temperatures of approximately 700°C and pressures of approximately 3 kbar. Progressive deformation, indicated by porphyroblast-matrix relationships, are interpreted to be a result of minor displacements of the country rock associated with and facilitated by intrusion of the Glenlyon Batholith, followed by static heating. Isolated skarn units exist along contacts between the batholith and its wall rocks. A skarn unit is also present along a nearby north-northeast-trending dextral strike-slip fault that predates and is intruded by the batholith.

RÉSUMÉ

Les roches calcaireuses du Paléozoïque précoce du terrane de Cassiar sont recoupées par le batholite de Glenlyon du Crétacé précoce. La géothermobarométrie des roches encaissantes, utilisant les assemblages grenat - biotite et grenat - biotite - muscovite - aluminosilicate - quartz, indique un métamorphisme du faciès des amphibolites inférieures et des températures et pressions d'environ 700°C et 3 kbar, respectivements. La déformation progressive enregistrée dans les relations de fabriques entre les porphyroblastes et la matrice sont vraisemblablement le résultat d'un déplacement mineur le long de la marge du batholite suivi d'un réchauffement statique. Des indices de skarn forment des affleurement isolés le long du contact entre le batholite et les roches encaissantes, de même que le long d'une faille de décrochement dextre d'orientation nord-nord-est qui est recoupée par le batholite.

[1]*billyroc@uvic.ca*

[2]*kaesy@uvic.ca*

[3]*stj@uvic.ca*

[4]*Box 3055, Stn. CSC, Victoria, British Columbia, Canada V8W 3P6*

INTRODUCTION

Miogeoclinal rocks of Cassiar Terrane, in southeastern Glenlyon map area (105L), occur in a narrow northwest-striking belt between the western margin of the Early Cretaceous Glenlyon Batholith and the Tummel fault zone, which separates Cassiar Terrane from allochthonous rocks of the Yukon-Tanana Terrane (Fig. 1; Colpron et al., 2002; Gladwin et al., 2002; Campbell, 1967).

During intrusion of the batholith, platformal to basinal rocks of Cassiar Terrane were extensively metamorphosed, developing pods of lead-zinc skarn mineralization in marble (Lokken occurrence, Yukon MINFILE, 2001, 105L 001). Some exploration work has been done on the Lokken occurrence (Doherty, 1991; Doherty 1996), but little documentation of its geology and the conditions during contact metamorphism has been recorded.

This paper presents the results of detailed (1:20 000 scale) geological mapping and geothermobarometric studies from a 25 km^2 area around the Lokken occurrence. This study was conducted as part of a larger regional mapping program (Yukon Targeted Geoscience Initiative (TGI), Fig. 1; Colpron et al., this volume) and in concert with more extensive detailed mapping of the Truitt Creek area (Gladwin et al., 2002; this volume).

GEOLOGY

CASSIAR TERRANE

Rocks west of the Glenlyon Batholith are calcareous pelite and carbonate, interbedded with calc-silicate rocks and minor amphibolite of the Cassiar Terrane (Gordey and Makepeace, 2001). Originally mapped by Campbell (1967), these rocks were assigned to the Middle Cambrian (and younger ?) Harvey Group. On a recent compilation, Gordey and Makepeace (2001) incorporated the Harvey Group within the Upper Proterozoic-Lower Cambrian Ingenika Group (Windermere Supergroup).

Regional mapping north of the study area has reinterpreted these rocks as higher grade equivalents of the Cambrian-Ordovician Kechika Group and Silurian-Devonian Askin Group (Gladwin et al., 2002; this volume; Colpron et al., 2002; this volume). In addition, this mapping indicates that much of the area Campbell (1967) thought was underlain by metasedimentary rocks is actually underlain by granitic rocks of the Glenlyon Batholith (Gladwin et al., 2002). In the study area (Fig. 2), metasedimentary rocks of the Cassiar Terrane have been contact-metamorphosed to amphibolite facies. Six mappable units are recognized in the area. They vary from coarse-grained, metaclastic rocks of the Kechika

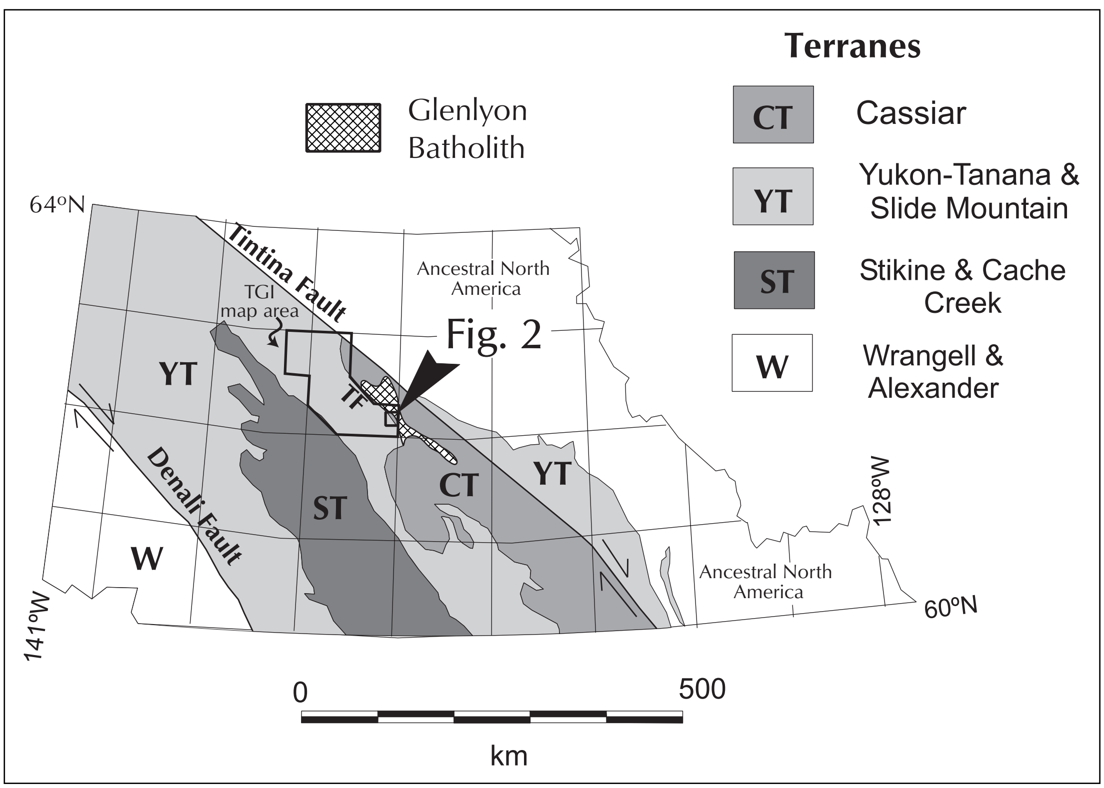

__Figure 1.__ Simplified regional geological map of the southern Yukon (modified after Wheeler and McFeely, 1991). The study area (indicated by the Figure 2 box) is located near the Tummel Fault (TF) at the western margin of the Cassiar Terrane.

Group at the bottom of the section to fine-grained calcareous rocks of the Askin Group at the top. Compositional layering is parallel to the dominant schistosity, which strikes northwest and dips moderately to the southwest.

The Kechika Group in the area consists of five mappable units. The structurally lowest unit (MBa) consists of brown, rusty-weathering, quartz-muscovite-biotite schist, which forms layers up to 50 m thick. Near the margin of Glenlyon Batholith, the schist is deformed by irregular folds that have amplitudes of 30-50 cm. These folds are mimicked by a 5-cm-thick sill of muscovite pegmatite, and are interpreted to have been produced by intrusion of the batholith. Minor amounts of coarsely recrystallized marble contain < 5% evenly distributed biotite flecks that are aligned parallel to the dominant foliation. Foliated amphibolite sills occur locally. They are generally parallel to the schistosity, but locally cut across the schistosity and compositional layering at low angles. Green quartzite layers <2 m thick, rare, medium-grained garnet-wollastonite-diopside calc-silicate schist, and gneiss are also included within this unit. Unit Mba also occurs as pendants that occupy topographic high points within the Glenlyon Batholith. Rocks within these pendants exhibit an intense alteration, and layering is discordant with the regional structural trend outside of the batholith.

A unit (MBbm) of tan- to grey-weathering, coarsely crystalline, impure marble (± diopside) is repeated three times in the area (Fig. 2). It is up to 60 m thick and comprises calc-silicate layers (up to 30% of the unit) and minor amounts of quartz-biotite-muscovite schist. Marble layers commonly include amphibolite sills up to 2 m thick that are boudinaged and folded with the surrounding layers.

A unit (MBbs) of foliated, medium-grained, light grey to brown biotite-quartz schist (± cordierite ± andalusite) is repeated twice with the underlying marble unit (MBbm). It also includes significant amounts of quartz-mica schist, minor coarsely recrystallized pelitic marble (± diopside), minor amphibolite, and rare calcareous quartz-plagioclase pebble metaconglomerate. The biotite-quartz schist (unit MBbs) contains less than 10% feldspar, and is crenulated. Two horizons of pebble metaconglomerate occur above and below a 100-m-thick succession of quartz-mica schist and marble. The lower metaconglomerate horizon (at least 1 m thick) is well sorted, with oblate pebbles 3-6 cm in diameter. The upper horizon of metaconglomerate is well sorted and contains smaller pebbles (2-3 cm in diameter).

Unit MBc is dominated by green to white, medium-grained, plagioclase-diopside ± garnet ± wollastonite calc-silicate gneiss and schist, coarse crystalline pelitic marble and minor amphibolite. This unit overlies the westernmost occurrence of marble of unit MBbm (Fig. 2). Calc-silicate layers up to 80 m thick show cm-scale compositional layering defined by green and white banding of diopside-rich and quartz-plagioclase-wollastonite-dominated layers, respectively. A unit of rusty brown to gold, medium-grained garnet-biotite-muscovite schist, with minor plagioclase-diopside calc-silicate schist and coarsely crystalline marble (MBab) occurs above the calc-silicate unit (MBc; Fig. 2). This unit contains 1-4 mm poikiolitic garnet porphyroblasts with quartz inclusion trails.

A medium- to coarse-grained, medium grey marble, unit MBd, with numerous calcite veins is the westernmost unit, adjacent to the Tummel fault zone. This marble is compositionally homogeneous and lacks the significant siliciclastic component observed in the marble unit MBbm. It is assigned to the Askin Group (Gladwin et al., 2002; Colpron et al., 2002).

GLENLYON BATHOLITH

More than half (>12 km^2) of the study area is underlain by the Glenlyon Batholith (Fig. 2). It is characterized by three comagmatic felsic phases (Fig. 3): (a) muscovite pegmatite, (b) biotite-muscovite ± hornblende granite, and (c) ± hornblende-biotite granodiorite. All phases are characterized by a weak planar foliation that is interpreted as a magmatic fabric.

The muscovite-biotite + hornblende granite is grey, equigranular to porphyritic, medium- to coarse-grained, with 5-10% muscovite. Plagioclase megacrysts up to 4 cm long are locally present. This phase is common in the northern part of the study area and exists as rare apophyses in the country rock. The granite is interpreted to be the oldest phase of the intrusion as it is cut by both the granodiorite and the pegmatite. A single outcrop of moderately foliated muscovite-biotite granite occurs at the margin of the batholith. This foliated granite is metamorphosed to chlorite grade (lower greenschist facies) and has a foliation consisting of aligned chlorite grains <0.5 mm long, concordant with the regional structural trend. This foliated granite is interpreted as an early phase of the batholith that was partially cooled and subsequently deformed and metamorphosed during intrusion of the main phases of the batholith.

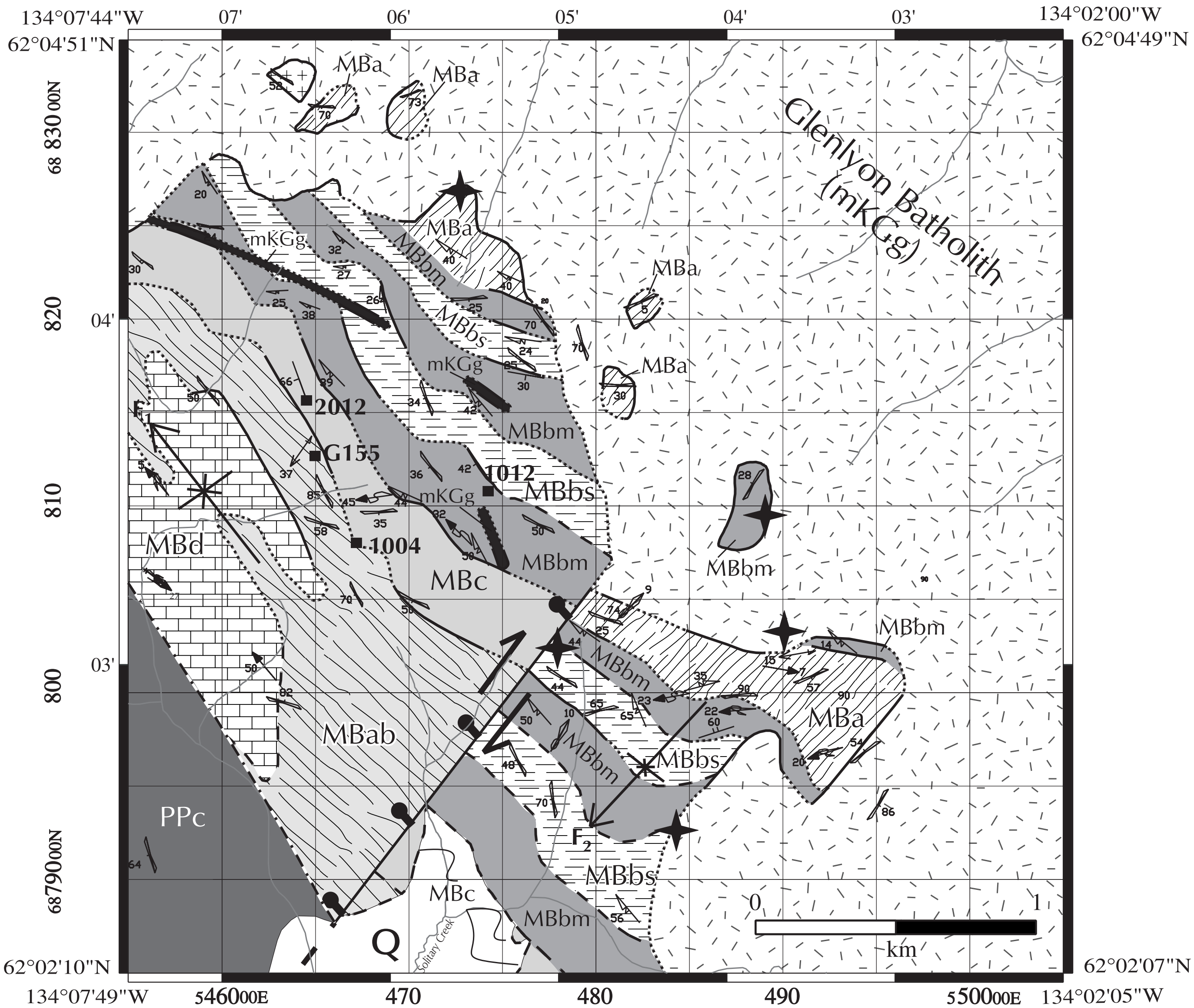

Figure 2. *Geological map of the study area. The locations of geothermobarometry samples are indicated by black squares. Labels correspond to the last 4 digits of the sample numbers. Legend on opposite page.*

The biotite granodiorite is pink-weathering, equigranular, medium- to coarse-grained and leucocratic with <5% biotite. This is the most voluminous phase of the batholith, and rarely occurs as dykes. Contacts between the granodiorite and granite phases are undulatory (Fig. 3) and gradational, indicating a comagmatic relationship.

The granite pegmatite occurs as apophyses in country rock and as dykes within the batholith. Pegmatite veins and dykes are characterized by 3-5 cm muscovite booklets. Pegmatite veins cut and are younger than the more equigranular granite and granodiorite phases of the batholith. Pegmatite, however, locally grades into more equigranular muscovite granite, indicating that the pegmatite veins are probably a late stage melt of the batholith and not the products of a younger magmatic event.

The batholith intrudes older Paleozoic continental margin rocks of Cassiar Terrane. A single K/Ar whole rock age determination of 105 ± 4 Ma (Hunt and Roddick, 1990) from north of Robert Campbell highway indicates an Early Cretaceous age for the Glenlyon Batholith.

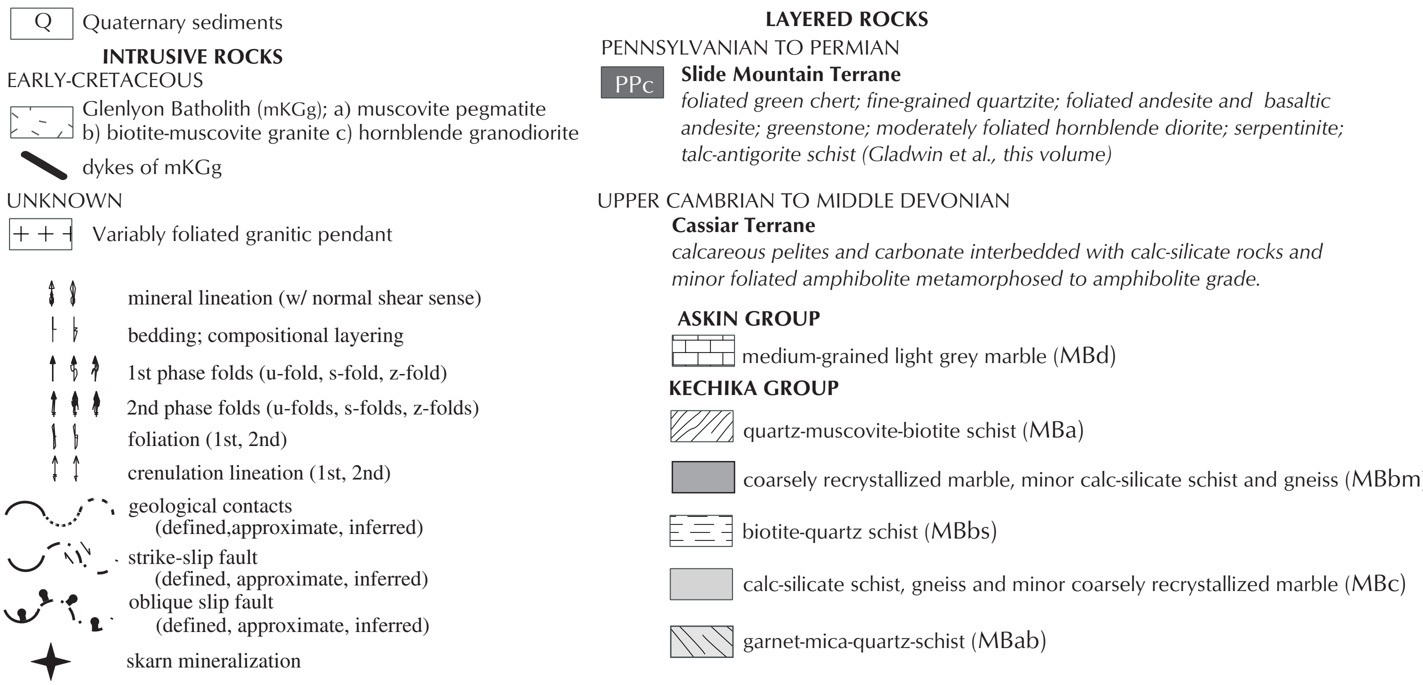

Figure 2. *Legend for map on preceeding page.*

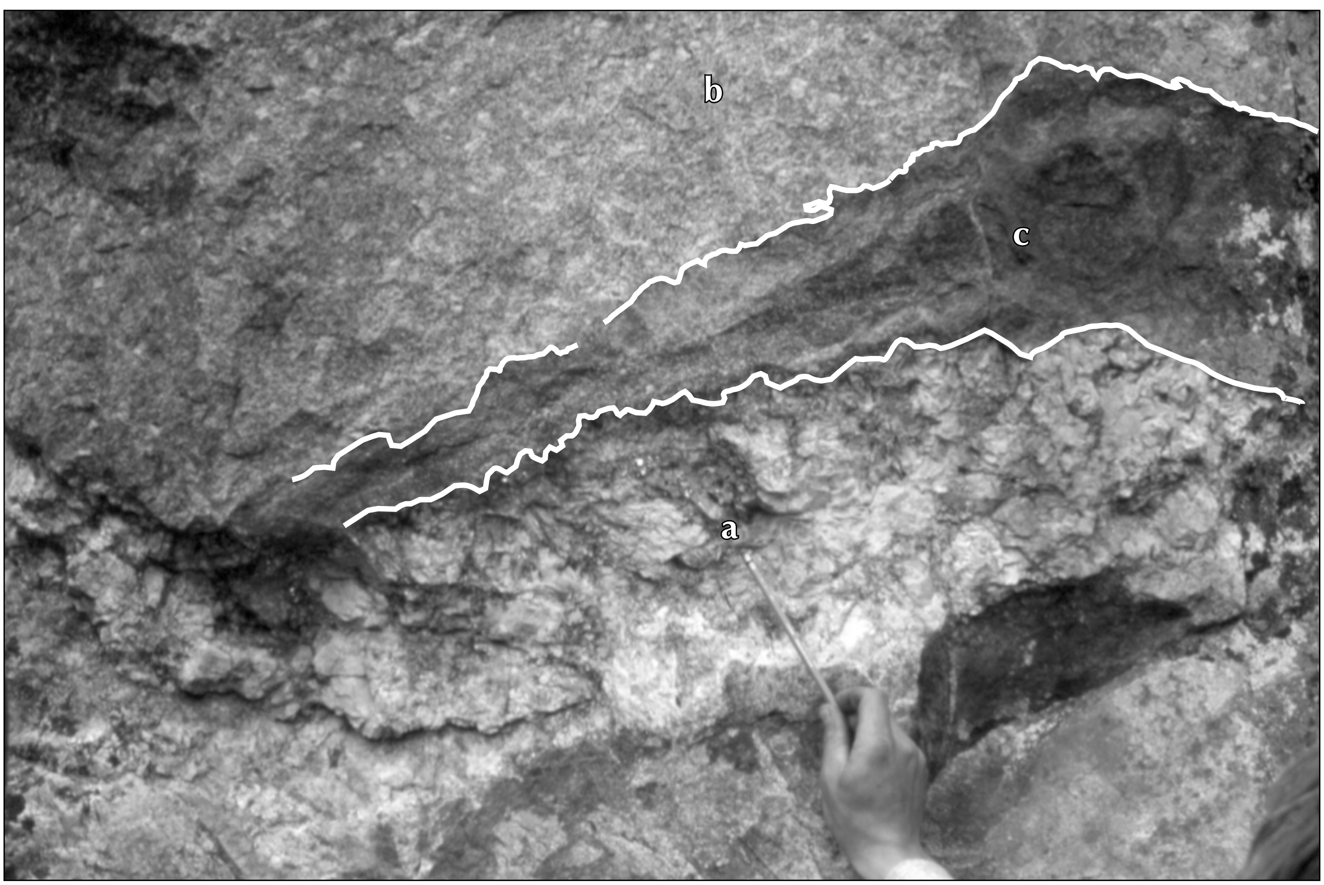

Figure 3. *The three phases of the Glenlyon Batholith:* ***(a)*** *muscovite pegmatite,* ***(b)*** *biotite-muscovite granite and* ***(c)*** *hornblende-biotite granodiorite. The upper two phases share an embayed contact suggesting comagmatism.*

STRUCTURAL GEOLOGY

Two phases of deformation are evident in rocks of the Cassiar Terrane. The first produced a north-northwest-striking, west-dipping, layer-parallel foliation defined by micas in the schists (S_1). The foliation is axial planar to tight folds (F_1) that plunge 23°-43° to the northwest (Fig. 4a,b). First phase structures are dominant and define the structural trend in the area. The second phase of deformation includes 1) the development of a northeast-striking oblique-slip fault, 2) the formation of broad open wrinkles in the phase one schistosity, and 3) the development of open, moderately west-plunging folds (Fig. 4c). The second phase open folds (F_2) deform the dominant foliation and locally modify the regional structural trend such that it is nearly parallel with second phase fold axes (Fig. 2). Compositional layering, defined by 1-2 cm thick siliciclastic layers in marble and 2-3 cm thick diopside-quartz layers in calc-silicate rock, converges at low angles to the S_1 foliation and is interpreted to represent transposed bedding. The foliation commonly parallels the intrusive margin near the batholith, locally creating push folds with amplitude of 30-50 cm. A northeast-striking fault in the study area has a net dextral strike separation of 1 km. The fault is truncated to the southwest by the Tummel fault zone (Gladwin et al., this volume) and to the northeast by the Glenlyon Batholith.

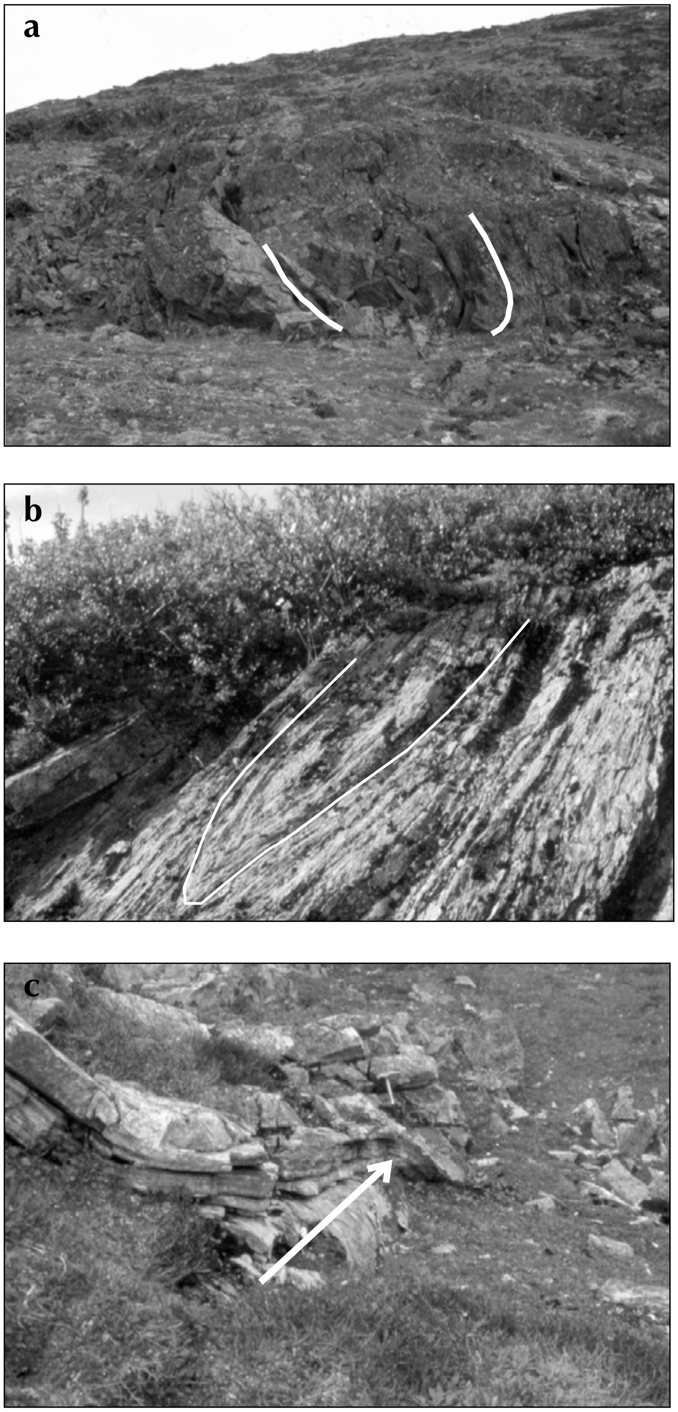

Figure 4. ***(a)*** *F_1 fold view looking up plunge. The fold is closing to the northeast and plunging slightly to the northwest in southern map area. Field of view is approximately 20 m.* ***(b)*** *View looking down plunge of F_1 fold in the northern part of the map area. Field of view is approximately 4 m.* ***(c)*** *West-plunging broad open F_2 fold; hammer for scale. The arrow points down plunge.*

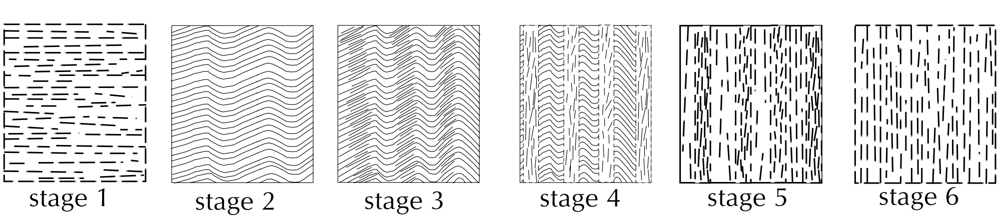

Figure 5. *The six stages of cleavage development (after Bell and Rubenach, 1983).*

METAMORPHISM

Contact aureole mineral assemblages overprint a regional greenschist facies fabric. Porphyroblast inclusion trails preserve earlier schistosities frozen during progressive deformation (Bell & Rubenach, 1983; Olesen, 1978; Vernon, 1978). Bell and Rubenach (1983) identified six stages defined by the geometry of the matrix fabric (S_e) during the development of a new schistosity (Fig. 5). Internal fabrics (S_i) may capture one or several stages of secondary schistosity development. The terminology of Bell and Rubenach (1983) is used here. Foliated rocks in this study area exhibit a stage 5 S_e observable in all lithologies. Locally, porphyroblasts have captured stages 2 to 4 of foliation development.

Brown to burgundy, 1-4 mm diameter, almandine-rich garnet porphyroblasts are abundant in unit MBab. The garnets are subhedral to anhedral, with quartz inclusions (S_i) preserving stages 2 to 4 of schistosity development (Figs. 6a,b). S_i fabric is continuous through the core of the

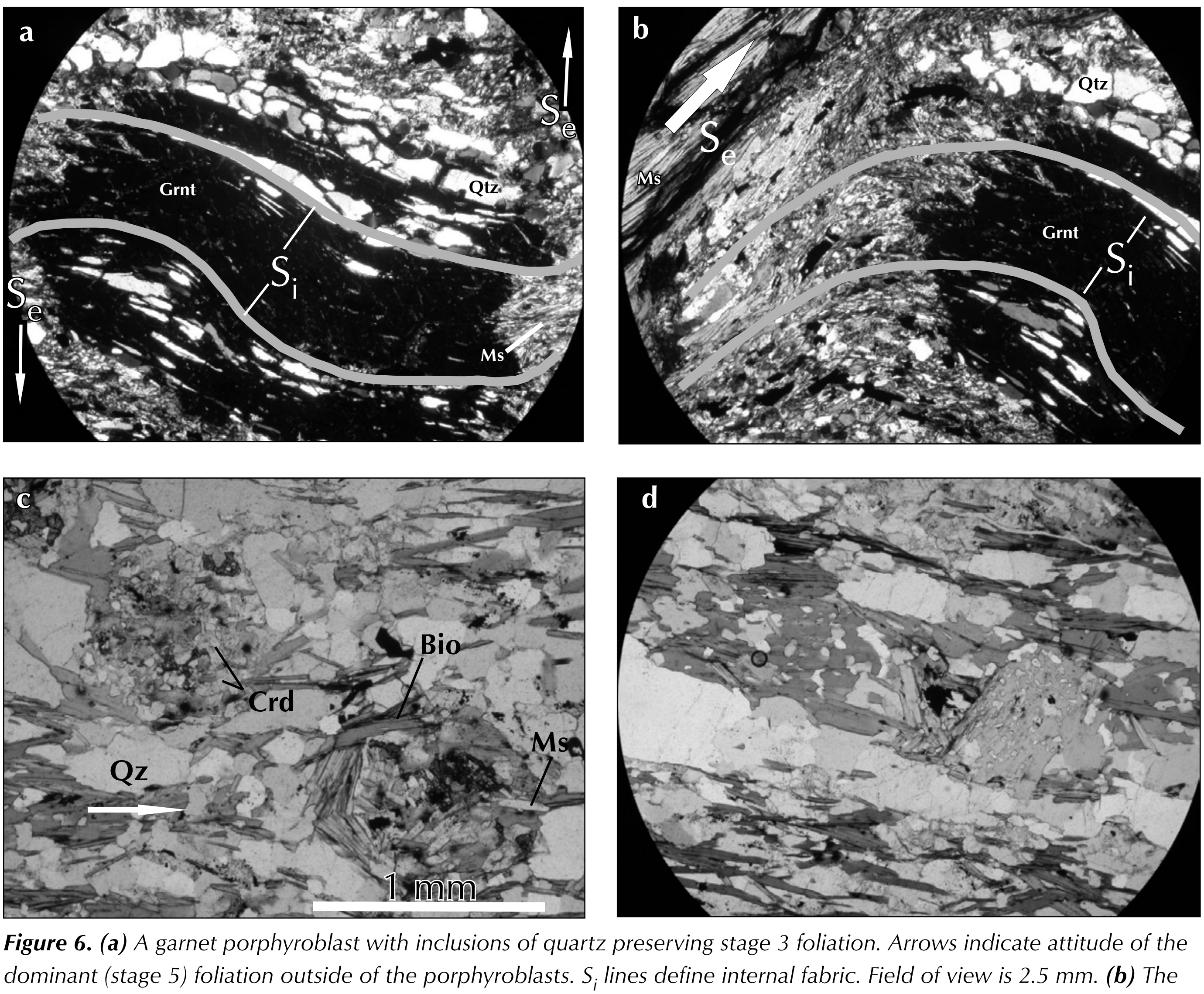

Figure 6. ***(a)*** *A garnet porphyroblast with inclusions of quartz preserving stage 3 foliation. Arrows indicate attitude of the dominant (stage 5) foliation outside of the porphyroblasts.* S_i *lines define internal fabric. Field of view is 2.5 mm.* ***(b)*** *The same garnet showing an inclusion trail emerging from garnet and bending into alignment with biotite-muscovite foliation. White arrow indicates dominant foliation; grey lines follow inclusion trails within garnet. Field of view is 2.5 mm.* ***(c)*** *Biotite-quartz-cordierite-tourmaline aggregates growing across the foliation.* ***(d)*** *Late growth biotite porphyroblast developed across the foliation. Field of view is 2.5 mm. Photomicrographs taken at 4x magnification.*
And – andalusite; Bio – biotite; Crd – cordierite; Grnt – garnet; Ms – muscovite; Qtz – quartz.

Table 1. *Electron microprobe mineral analysis results.*

Sample	Ox% (Na)	Ox% (Mg)	Ox% (Al)	Ox% (Si)	Ox% (K)	Ox% (Ca)	Ox% (Ti)	Ox% (Cr)	Ox% (Mn)	Ox% (Fe)	Ox% (Ba)	Wt% (F)	Wt% (Cl)	total
Garnet														
RB004-1	0.04	1.53	21.39	36.52	–	9.63	0.14	0.01	0.66	29.09	–	–	–	99.02
RB004-2	0.03	1.16	21.43	37.11	–	9.93	0.17	0.00	0.80	29.55	–	–	–	100.18
RB004-3	0.03	1.03	21.33	36.80	–	10.00	0.14	0.05	1.27	29.04	–	–	–	99.68
RB004-4	0.05	1.10	21.54	37.10	–	9.78	0.14	0.02	1.16	29.85	–	–	–	100.76
KG155-1	0.00	1.52	21.46	36.55	–	8.80	0.09	0.07	0.63	30.70	–	–	–	99.83
KG155-2	0.01	1.28	21.43	36.88	–	9.23	0.11	0.00	0.80	30.42	–	–	–	100.16
KG155-3	0.01	1.31	21.44	36.47	–	8.92	0.12	0.00	0.75	30.44	–	–	–	99.48
KG155-4	0.02	1.22	21.40	37.05	–	9.33	0.08	0.01	0.84	29.89	–	–	–	99.83
KG155-5	0.04	0.99	21.53	36.87	–	9.27	0.11	0.03	2.69	28.55	–	–	–	100.09
KG155-6	0.03	0.97	21.30	36.62	–	9.54	0.13	0.01	2.88	28.09	–	–	–	99.57
RB02012-1	0.03	2.37	21.58	37.04	–	7.12	0.09	0.04	0.30	31.64	–	–	–	100.22
RB02012-2	0.01	1.85	21.41	37.12	–	7.15	0.07	0.00	0.28	32.40	–	–	–	100.30
RB02012-3	0.04	1.19	21.07	36.89	–	8.30	0.09	0.01	1.93	30.68	–	–	–	100.21
RB02012-4	0.01	1.11	21.25	36.77	–	8.72	0.11	0.01	2.53	29.90	–	–	–	100.40
RB02012-7	0.00	2.12	21.66	36.98	–	6.44	0.08	0.02	0.25	32.90	–	–	–	100.46
RB02012-8	0.02	1.63	21.27	36.87	–	6.99	0.04	0.04	0.54	32.54	–	–	–	99.93
RB02012-9	0.04	1.12	21.24	37.05	–	8.77	0.11	0.00	2.39	29.96	–	–	–	100.67
RB02012-10	0.01	1.36	21.46	36.96	–	7.97	0.09	0.00	0.95	31.36	–	–	–	100.16
Pyroxene														
RB01004-1	0.08	8.61	0.37	51.20	–	23.57	0.00	0.02	0.22	14.99	–	–	–	99.06
RB01004-2	0.09	9.22	0.33	51.05	–	23.71	0.00	0.01	0.27	14.99	–	–	–	99.66
RB01004-3	0.08	9.43	0.25	51.52	–	23.40	0.04	0.02	0.30	14.42	–	–	–	99.46
RB01004-4	0.09	9.47	0.22	51.25	–	23.31	0.01	0.02	0.31	14.30	–	–	–	98.99
Biotite														
KG155-1	0.15	7.53	17.34	35.12	9.40	0.05	2.50	0.07	0.21	23.29	0.18	0.48	0.10	95.85
KG155-2	0.13	7.51	17.47	34.81	9.19	0.07	2.39	0.07	0.19	23.56	0.20	0.47	0.18	95.60
KG155-4	0.05	9.05	18.01	32.49	6.36	0.08	1.44	0.00	0.26	25.54	0.12	0.33	0.15	93.50
KG155-6	0.18	8.45	19.23	36.13	9.87	0.00	2.43	0.06	0.22	20.04	0.12	0.45	0.08	96.74
KG155-7	0.12	8.45	19.20	36.11	9.87	0.00	2.34	0.00	0.18	20.10	0.01	0.43	0.07	96.47
KG155-10	0.05	6.32	20.90	33.20	8.81	0.05	0.69	0.03	0.19	24.47	0.03	0.24	0.13	94.74
RB02012-1	0.23	7.67	19.21	35.84	9.63	0.03	2.79	0.00	0.07	20.46	0.04	0.25	0.00	95.99
RB02012-2	0.16	7.78	19.38	35.98	9.83	0.00	2.82	0.04	0.06	20.67	0.05	0.31	0.01	96.78
RB02012-5	0.24	8.56	18.61	35.76	9.65	0.00	2.98	0.03	0.08	20.24	0.11	0.34	0.05	96.26
RB02012-6	0.23	8.74	18.38	36.54	9.64	0.00	2.95	0.05	0.07	19.46	0.02	0.40	0.00	96.07
RB02012-9	0.14	5.76	18.87	34.82	9.48	0.00	3.22	0.07	0.12	23.75	0.11	0.11	0.00	96.34
RB02012-10	0.13	5.64	19.21	34.75	9.67	0.00	3.22	0.06	0.16	23.48	0.08	0.21	0.03	96.40
Feldspar														
KG155-1	5.52	0.00	28.47	55.79	0.01	10.52	–	–	–	0.32	–	–	–	100.72
KG155-2	6.17	0.00	27.20	57.33	0.14	9.06	–	–	–	0.08	–	–	–	99.98
KG155-3	5.77	0.00	27.63	56.20	0.14	9.93	–	–	–	0.01	–	–	–	99.77
RB02012-3	6.09	0.00	27.42	57.62	0.26	9.37	–	–	–	0.03	–	–	–	100.79
RB02012-4	5.81	0.01	27.86	56.36	0.24	9.96	–	–	–	0.05	–	–	–	100.28
White Mica														
KG155-8	0.40	0.04	18.45	65.47	16.27	0.00	0.02	0.02	0.00	0.25	0.27	0.00	0.01	101.20
KG155-9	0.40	0.03	18.50	65.77	16.43	0.02	0.00	0.00	0.04	0.41	0.16	0.00	0.00	101.75
RB02012-3	0.44	1.18	33.54	47.52	10.26	0.01	0.74	0.03	0.01	1.61	0.21	0.13	0.01	95.55
RB02012-4	0.41	1.00	33.41	46.52	9.78	0.02	0.56	0.01	0.00	1.24	0.26	0.14	0.04	93.22
RB02012-7	0.46	0.87	34.84	45.90	10.53	0.00	0.49	0.04	0.07	1.49	0.31	0.06	0.00	95.01
RB02012-8	0.50	1.21	33.54	46.71	10.57	0.01	0.52	0.04	0.00	1.52	0.22	0.15	0.01	94.84

Ox: oxide; Wt: weight

garnets to the rims where it emerges at the anhedral garnet boundary and is incorporated into a muscovite-biotite fabric that bends into alignment with S_e. Stage 3 is the most commonly observed relict schistosity and is interpreted to be synchronous with the peak of garnet growth.

Aggregates of biotite-quartz-cordierite ± tourmaline, <1 mm in diameter in biotite-quartz schist of unit MBbs are common (Fig. 6c). Locally, garnets occur within the aggregates as anhedral masses in disequilibrium with surrounding minerals and are interpreted to be retrograded garnet pseudomorphs. Biotite in these aggregates typically has metamict haloes around zircon inclusions. S_e is defined by biotite and is locally included within porphyroblasts, but more commonly displays a weak wrap-around texture that implies late development of the biotite-quartz-cordierite porphyroblasts (with respect to development of the main schistosity).

Post-kinematic contact metamorphism affects the entire study area. It is most commonly characterized by late-developing <1 mm biotite porphyroblasts that grow across a well defined biotite ± muscovite foliation in units MBa and MBbs (Fig. 6d). Further from the batholith, smaller <0.2 mm muscovite porphyroblasts in garnet-

Table 2. *Summary of mineral assemblages, thermometers and barometers used, and calculated P-T.*

Sample no.	Rock name	Mineralogy	Thermometer/ Barometer used	Calculated T (°C)	Calculated P (kPa)
KG01-155	garnet-biotite-muscovite-schist	quartz, muscovite, biotite, almandine, albite, andalusite, tourmaline	garnet-mica-aluminosilicate, garnet-biotite	738	3.1
RB01-004	garnet calc-silicate schist	almandine, diopside, calcite, sphene, epidote, plagioclase	garnet-diopside	577	–
RB01-012	knotted biotite schist	quartz, muscovite, biotite, almandine, albite, andalusite, cordierite, tourmaline, chlorite	garnet-mica-aluminosilicate, garnet-biotite	661	2.7
RB02-012	garnet-biotite-muscovite-schist	quartz, almandine, muscovite, biotite, albite, chlorite	garnet-biotite	721	–

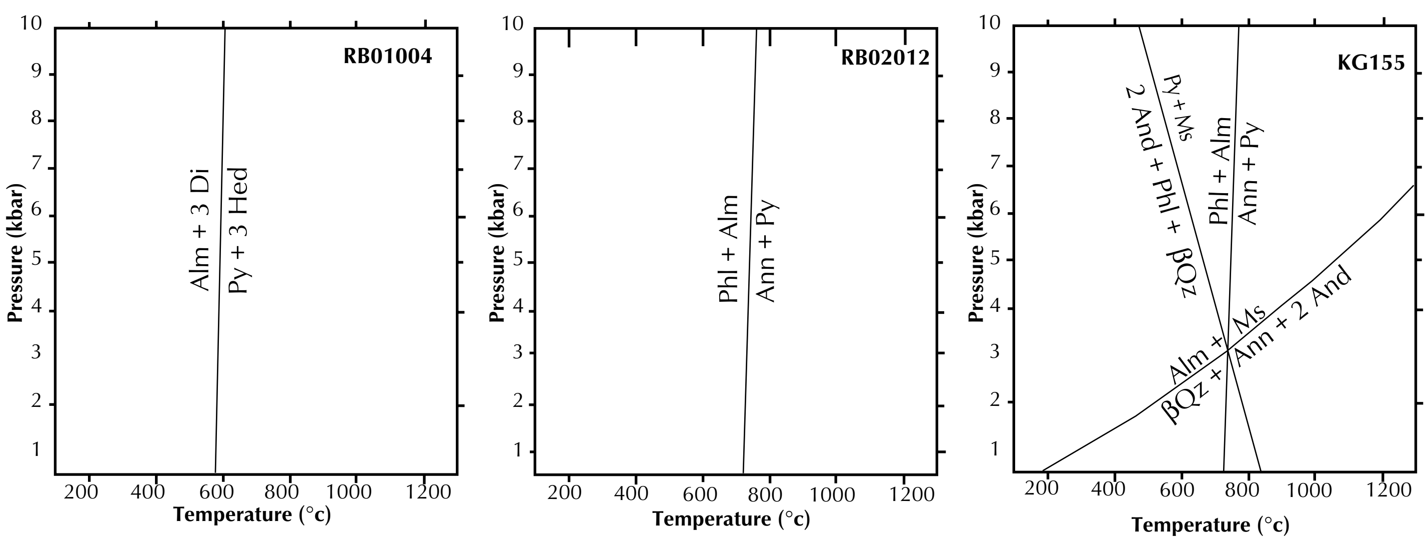

Figure 7. *Pressure-temperature plots constructed using TWEEQU software (Berman, 1991). Alm – almandine; Di – diopside; Py – pyrope; Hed – hedenbergite; βQz – beta-quartz; Ms – muscovite; Phl – phlogopite; Ann – annite; And – andalusite.* ***(a)*** *Univariant Fe-Mg exchange reaction from a calc-silicate schist 1300 m from the batholith, resulting in a temperature of 590°C.* ***(b)*** *Univariant garnet-biotite Fe-Mg exchange reaction from a garnet-mica schist taken 1100 m from the batholith's margin. A temperature of 730°C is extrapolated at 3 kbar.* ***(c)*** *Garnet-biotite-aluminosilicate-quartz and garnet-biotite exchange reactions from a garnet-mica schist 1380 m from the intrusive margin. Results indicate a pressure of 3.1 kbar and a temperature of 738°C. This sample is considered representative of the pressure and temperature conditions achieved during emplacement of the Glenlyon Batholith. Sample locations shown on Figure 2.*

muscovite-biotite-quartz schists of unit MBab grow across the dominant biotite-muscovite foliation. The biotite porphyroblasts commonly include zircon and quartz; the muscovite locally includes tourmaline. Both the muscovite and biotite porphyroblasts are oriented randomly, defining no coherent foliation and are interpreted to be post-kinematic thermal metamorphism.

Gladwin et al. (this volume) show that contact metamorphism associated with Glenlyon Batholith affect rocks up to 10 km west of the batholith.

GEOTHERMOBAROMETRY

Analyses were obtained using wavelength dispersive analysis on the Cameca SX-50 electron microprobe at the University of British Columbia. The data was collected as oxide percentages (Table 1), reduced, and P-T plots (Fig. 7) were constructed using the thermobarometric database and software of Berman (1991). Geothermobarometry results are shown in Fig. 7 and summarized in Table 2.

Samples of metapelite with garnet + biotite + quartz + muscovite + plagioclase + cordierite + andalusite, and calc-silicate rocks with garnet + clinopyroxene + quartz mineral paragenesis were selected for microprobe analysis (Table 2). The garnet-biotite thermometer of Berman (1991) and solid solution models of Berman and Aranovich (1996) for garnet and biotite were used. Pressure was determined using the net transfer equilibria reaction for biotite-garnet-muscovite-quartz-aluminosilicate (Ghent and Stout, 1981) and the solid solution models of Chatterjee and Froese (1975) for mica and Berman et al. (1995), and Berman and Aranovich (1996) for garnet and biotite.

Pressure and temperature estimates based on microprobe analysis suggest low pressure amphibolite facies metamorphic conditions in the aureole of the Glenlyon Batholith. Pressure estimates of 3.1 kbar and temperatures of 570° C and 720°C were derived from microprobe analyses. These results are consistent with the lower amphibolite facies metamorphism indicated by metamorphic mineral assemblages, and the presence of cordierite and andalusite in metapelites of the Cassiar Terrane adjacent to the Glenlyon Batholith.

MINERALIZATION AT THE LOKKEN OCCURRENCE

Pods of lead-zinc-silver skarn mineralization occur at the contact between the Glenlyon Batholith and marble horizons (Fig. 2; Yukon MINFILE, 2001, 105L 001). A single occurrence along the north-northeast striking oblique fault was also noted. Suphide minerals consist of disseminated to massive sphalerite, galena and pyrite with associated diopside, garnet, actinolite, calcite and quartz (Doherty, 1996). Layers of marble can be clearly followed into the margin of the batholith where the carbonate has been replaced by mineralization. This implies the mineralization is attributable to the intrusion of the Glenlyon Batholith. If mineralization is a product of the intrusion then the pressure and temperature constraints on metamorphism must also constrain the mineralization event. A single locality of mineralization in the north of the study area occurs in unit MBa on the intrusive contact. Chlorite, quartz and muscovite mineral paragenesis at this site indicate low temperature metamorphism (Winkler, 1979). This is interpreted to be a result of replacement of earlier minerals by infiltration of meteoric waters.

DISCUSSION

The Glenlyon Batholith was intruded syn- to post-kinematically, as indicated by inclusion trails within garnet porphyroblasts and chlorite metamorphism in the earliest phase of intrusion. Biotite-quartz-cordierite porphyroblasts display both syn-kinematic and post-kinematic growth features. Strain during intrusion of the batholith was accommodated by local push folds at the margin and development of a margin parallel schistosity. Displacement at the margin of the batholith is interpreted to be minimal due to lack of significant foliation within the batholith, and it likely occurred during emplacement of the earliest phases of the intrusion. Randomly oriented biotite and muscovite porphyroblasts growing across foliation show that metamorphism continued after the cessation of strain, further enhancing schistosity in the wall rocks. Rotated pendants of country rock that cap topographic high points are interpreted to have foundered into the magma during intrusion. A contact aureole imposed by the batholith extends up to 10 km away from the batholith (Gladwin et al., this volume).

Geothermobarometric results from calc-silicate schists and meta-pelites indicate that the country rocks to the Glenlyon Batholith were metamorphosed at 8 to 10 km depth and subject to temperatures between 570°C and 720°C. Higher than expected mineral formation temperatures are encountered in rocks over 1 km from the nearest surface expression of the batholith. This may indicate that the intrusion is present beneath these locations at relatively shallow depths, or may be due to circulation of abundant calcium-rich fluids. The results here are similar to those documented by Smith and Erdmer (1990) in country rock surrounding the Early Cretaceous Anvil Batholith near Faro, south-central Yukon. The Anvil Batholith is similar both in age and in composition, with three phases including muscovite-biotite granite, hornblende-biotite granodiorite, and minor granite intrusions. Rb-Sr whole rock ages of ~99 Ma for the hornblende-biotite granodiorite phase and ~100 Ma for the muscovite-biotite granite, and K/Ar crystallization ages of 81-102 Ma suggest an Early to mid-Cretaceous age for intrusion of the Anvil Batholith(Pigage and Anderson, 1985).

A mineral occurrence along a fault intruded by the Glenlyon Batholith indicates the fault may have acted as a conduit for migration of mineralizing fluids. Metamorphic conditions determined from wall rocks to the batholith suggest that mineralizing fluids were probably in excess of 600°C.

CONCLUSIONS

The Early Cretaceous Glenlyon Batholith consists of three coeval phases intruded syn- to post- kinematically into wall rocks of the Cassiar Terrane. Contact metamorphic mineral assemblages record pressures of ~3 kbar (8-10 km depth) and temperatures in excess of 600°C. Skarn mineralization developed near the intrusive margin during intrusion and development of the contact aureole. Similar results from other studies of Early Cretaceous batholiths and their aureoles may imply a unique intrusion style.

ACKNOWLEDGEMENTS

This study is part of a BSc honours thesis undertaken by the first author. Results are from two seasons of field work as part of a larger study in the Truitt Creek map area. Financial support was provided in part by the Yukon Geology Program and in part by the National Science and Engineering Council (NSERC) grant to S.T. Johnston. Helicopter transport was provided by Trans North Helicopters (Ross River) during the 2001 field season and Fireweed Helicopters during the 2002 field season. Operating assistance of the electron microprobe was provided by M. Raudsepp. The author acknowledges very beneficial discussions with Joe English, Steve Gordey, JoAnne Nelson and Maurice Colpron. A comprehensive review of the manuscript by Maurice Colpron was greatly appreciated.

REFERENCES

Bell, T.H. and Rubenach, M.J., 1983. Sequential porphyroblast growth and crenulation cleavage development during progressive deformation. Tectonophysics, vol. 92, p. 171-194.

Berman, R.G., 1991. Thermobarometry using multiequilibrium calculations: a new technique with petrologic applications. Canadian Mineralogist, vol. 29, p. 833-855.

Berman, R.G. and Aranovich, L.Y., 1996. Optimized standard state and solution properties of minerals; I. Model calibration for olivine, orthopyroxene, cordierite, garnet, and ilmenite in the system FeO-MgO-CaO-Al_2O_3-Ti_2-SiO_2. Contributions to Mineralogy and Petrology, vol. 126, no. 1-2, p. 1-24.

Berman, R.G., Aranovich, L.Y. and Pattison, D.R.M., 1995. Reassessment of the garnet-clinopyroxene Fe-Mg exchange thermometer; II, thermodynamic analysis. Contributions to Mineralogy and Petrology, vol. 119, no. 1, p. 30-42.

Campbell, R.B., 1967. Geology of Glenlyon map area, Yukon Territory (105/L1). Geological Survey of Canada Memoir 352, 92 p.

Colpron, M., Murphy, D.C., Nelson, J.L., Roots, C.F., Gladwin, K., Gordey, S.P., Abbott, G. and Lipovsky, P.S., 2002. Preliminary geological map of Glenlyon (105L/1-7,11-14) and northeast Carmacks (115I/9,16) areas, Yukon Territory (1:125 000 scale). Exploration and Geological Services Division, Yukon Region, Indian and Northern Affairs Canada, Open File 2002-9, and Geological Survey of Canada, Open File 1457.

Colpron, M., Murphy, D.C., Nelson, J.L., Roots, C.F., Gladwin, K., Gordey, S.P. and Abbott, J.G., 2003 (this volume). Yukon Targeted Geoscience Initiative, Part 1: Results of accelerated bedrock mapping in Glenlyon (105L/1-7, 11-14) and northeast Carmacks (115I/9,16) areas, central Yukon. *In:* Yukon Exploration and Geology 2002, D.S. Emond and L.L. Lewis (eds.), Exploration and Geological Services Division, Yukon Region, Indian and Northern Affairs Canada, p. 85-108.

Chatterjee, N.D. and Froese, E.F., 1975. A thermodynamic study of the pseudobinary join muscovite-paragonite in the system $KAlSi_3O_8$-$NaAlSi_3O_8$-Al_2O_3-SiO_2-H_2O. American Mineralogist, vol. 60, p. 985-993.

Doherty, A.R., 1991. Summary report on the Jack 1-64 claims. Report for Greater Lenora Resources Corporation, Mineral Resources Directorate, Yukon Region, Indian and Northern Affairs Canada, Assessment Report # 092926, 37 p.

Doherty, A.R., 1996. Report on the 1995 geological and geophysical exploration work on the Jack Property. Report for Greater Lenora Resources Corporation, Mineral Resources Directorate, Yukon Region, Indian and Northern Affairs Canada, Assessment Report #093386, 36 p.

Ghent, E.D. and Stout, M.Z., 1981. Geobarometry and geothermometry of plagioclase-biotite-garnet-muscovite assemblages. Contributions to Mineralogy and Petrology, vol. 76, p. 92-97.

Gladwin, K., Colpron, M. and Black, R., 2002. Geological map of Truitt Creek (NTS 105L/1), central Yukon (1:50 000 scale). Exploration and Geological Services Division, Yukon Region, Indian and Northern Affairs Canada, Open File 2002-5.

Gladwin, K., Colpron, M., Black, R. and Johnston, S.T., 2003 (this volume). Bedrock geology at the boundary between Yukon-Tanana and Cassiar terranes, Truitt Creek map area (NTS 105L/1), south central Yukon. *In:* Yukon Exploration and Geology 2003, D.S. Emond and L.L. Lewis (eds.) Exploration and Geological Services Division, Yukon Region, Indian and Northern Affairs Canada, p. 135-148.

Gordey, S.P. and Makepeace, A.J., (comps.), 2001. Bedrock Geology, Yukon Territory. Geological Survey of Canada, Open File 3754 and Exploration and Geological Services Division, Yukon Region, Indian and Northern Affairs Canada, Open File 2001-1, 1:1 000 000 scale.

Hunt, P.A. and Roddick, J.C., 1990. A compilation of K-Ar ages. Geological Survey of Canada, Report 19.

Olesen, N.O., 1978. Distinguishing between inter-kinematic and syn-kinematic porphyroblastesis. Geoloische Rundschau, vol. 67, p. 278-287.

Pigage, L.C. and Anderson, R.G., 1985. The Anvil plutonic suite, Faro, Yukon Territory. Canadian Journal of Earth Sciences, vol. 22, no. 8, p. 1204-1216.

Smith, J.M. and Erdmer, P., 1990. The Anvil aureole, an atypical mid-Cretaceous culmination in the northern Canadian Cordillera. Canadian Journal of Earth Sciences, vol. 27, p. 334-356.

Vernon, R.H., 1978. Porphyroblast-matrix relationships in deformed metamorphic rocks. Geologische Rundschau, vol. 67, p. 288-305.

Wheeler, J.O. and McFeely, P., 1991. Kinematic assemblage map of the Canadian Cordillera and adjacent parts of the United States of America. Geological Survey of Canada, Map 1712A, 1:2 000 000 scale.

Winkler, H.G.F., 1979. Petrogenesis of Metamorphic Rocks. 5th Edition, New York (Springer-Verlag).

Yukon MINFILE, 2001. Lokken – 105L 001. Exploration and Geological Services Division, Yukon Region, Indian and Northern Affairs Canada.